

Title	Different bioaugmentation regimes that mitigate ammonium/salt inhibition in repeated batch anaerobic digestion: Generic converging trend of microbial communities
Author(s)	Li, Zi Yan; Nagao, Shintaro; Inoue, Daisuke et al.
Citation	Bioresource Technology. 2024, 413, p. 131481
Version Type	VoR
URL	https://hdl.handle.net/11094/98336
rights	This article is licensed under a Creative Commons Attribution-NonCommercial-NoDerivatives 4.0 International License.
Note	

Osaka University Knowledge Archive : OUKA

<https://ir.library.osaka-u.ac.jp/>

Osaka University



Different bioaugmentation regimes that mitigate ammonium/salt inhibition in repeated batch anaerobic digestion: Generic converging trend of microbial communities

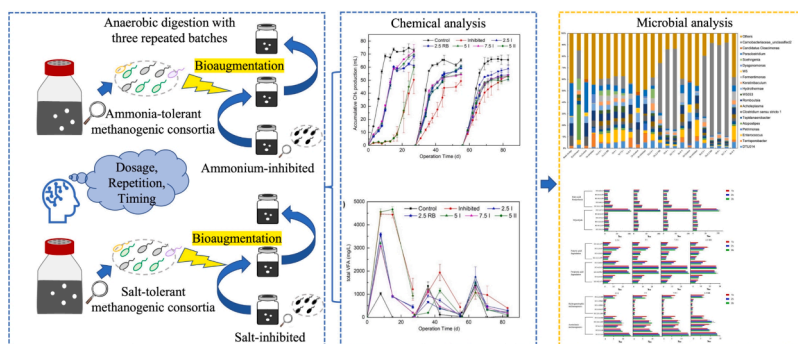
Zi-Yan Li, Shintaro Nagao, Daisuke Inoue, Michihiko Ike*

Division of Sustainable Energy and Environmental Engineering, Osaka University, 2-1 Yamadaoka, Suita, Osaka 565-0871, Japan

HIGHLIGHTS

- Bioaugmentation regimes that mitigate ammonia/salt inhibition in AD were evaluated.
- Positive correlation between reactor performance and inoculum dosage was temporary.
- Diminishing marginal effect occurred following repeated inoculum introduction.
- The archaeal community was not a key factor impacting performance change.
- A balanced and diversified bacterial community is key for active CH₄ production.

GRAPHICAL ABSTRACT



ARTICLE INFO

Keywords:
 Biogas recovery
 Inhibitory condition
 Inoculum dosing strategy
 Key enzyme prediction
 Deteriorated steady state

ABSTRACT

Bioaugmentation regimes (i.e., dosage, repetition, and timing) in AD must be optimized to ensure their effectiveness. Although previous studies have investigated these aspects, most have focused exclusively on short-term effects, with some reporting conflicting conclusions. Here, AD experiments of three consecutive repeated batches were conducted to determine the effect of bioaugmentation regimes under ammonium/salt inhibition conditions. A positive correlation between reactor performance and inoculum dosage was confirmed in the first batch, which diminished in subsequent batches for both inhibitors. Moreover, a diminishing marginal effect was observed with repeated inoculum introduction. While the bacterial community largely influenced the reactor performance, the archaeal community exhibited only a minor impact. Prediction of the key enzyme abundances suggested an overall decline in different AD steps. Overall, repeated batch experiments revealed that a homogeneous bacterial community deteriorated the AD process during long-term operation. Thus, a balanced bacterial community is key for efficient methane production.

* Corresponding author.

E-mail address: ike@see.eng.osaka-u.ac.jp (M. Ike).

<https://doi.org/10.1016/j.biortech.2024.131481>

Received 14 July 2024; Received in revised form 8 September 2024; Accepted 10 September 2024

Available online 12 September 2024

0960-8524/© 2024 The Author(s). Published by Elsevier Ltd. This is an open access article under the CC BY-NC-ND license (<http://creativecommons.org/licenses/by-nc-nd/4.0/>).

1. Introduction

Bioaugmentation is a promising technology for performance improvement/inhibition mitigation during the anaerobic digestion (AD) process (Duan et al., 2022; Li et al., 2023). Compared with other physical/chemical methods, bioaugmentation stands out with the merits of economic feasibility, rapid responses, and long-term stability (Li et al., 2023). Bioprocesses contributing to methane (CH₄) production are strengthened by exotic microorganisms introduced as bioaugmentation inocula; the effect may be further enhanced by the inoculum targeting weak steps (i.e., acetogenesis and methanogenesis) in the AD process or being pre-acclimated to specific inhibitors (Venkiteshwaran et al., 2016).

Ammonia and salt are ubiquitous inhibitors that cause performance deterioration and process imbalance in AD reactors, primarily originating from the ammonia-rich protein and nucleic acid degradation (Möller and Müller, 2012) and sodium ions used in food processing and pH adjustment (Grady et al., 1999). Various common feedstocks, such as animal manure (Fan et al., 2021), food waste (Jo et al., 2021), and municipal waste sludge (Chen et al., 2008), reportedly encounter single or combined inhibition by ammonia and salt when processed in AD reactors. Both inhibitors can severely weaken the activity of methanogens, particularly acetoclastic methanogens (Duc et al., 2023). Consequently, volatile fatty acids (VFAs), such as acetate and propionate, produced in the preceding steps of the AD process accumulate as intermediates to inhibit levels, further inhibiting the methanogenic community in a feedback loop, ultimately leading to process failure (Wang et al., 2015).

Recent attempts have been made to apply bioaugmentation to relieve ammonium/salt inhibition during AD. Li et al. (2017) investigated the effect of 45-d consecutive bioaugmentation with enriched cultures on mitigating ammonium inhibition at 3.0 g N L⁻¹. Results demonstrated bioaugmentation enhanced the average volumetric CH₄ production by approximately 50 mL L⁻¹ d⁻¹. In contrast, the non-bioaugmented reactor relatively failed and was recovered by the routine addition of bioaugmentation culture. Duc et al. (2023) also reported increased cumulative CH₄ production and mitigated VFAs accumulation after conducting one-time bioaugmentation (15 % on a volatile solid [VS] base) to mitigate salt inhibition under 30 g L⁻¹ of sodium chloride (NaCl). Meanwhile, unsuccessful bioaugmentation results were reported by Venkiteshwaran et al. (2016), revealing that the increased CH₄ production rate in the bioaugmented group was temporary and diminished after 8 d, even after administering a daily inoculum dose for ten consecutive days.

Considering the above situation, bioaugmentation in AD is still in a nascent stage, for which the regimes (i.e., dosage, repetition, and timing) must be optimized to ensure its effectiveness. Although previous studies have investigated the optimal dosage and meliority of single or routine dosing, most have focused exclusively on short-term effects (Duc et al., 2023; Linsong et al., 2022) and some have reached conflicting conclusions (Lee et al., 2022; Yang et al., 2016). Thus, with previous research failed to form a clear perspective, this study aimed to provide a comprehensive understanding of the influence of different bioaugmentation regimes on reactor performance, considering dosage, repetition, and timing of bioaugmentation simultaneously, by conducting model AD processes. Furthermore, to assess the sustainability of each bioaugmented group as well as the general patterns across inhibitor types, all AD processes were conducted in three consecutive batches lasting over 80 d under ammonia- and salt-inhibited conditions. The microbial community transition of different bioaugmentation regimes was analyzed to provide a microbial perspective using 16S rRNA amplicon sequencing. Conclusions on the efficacy of the different bioaugmentation regimes were made by analyzing two independent sets of data from both ammonia and salt inhibitors.

2. Material and methods

2.1. Feedstock, seed sludge, and bioaugmentation inoculum

Synthetic wastewater comprising glucose (2.3 g L⁻¹), yeast extract (1.1 g L⁻¹), peptone (0.9 g L⁻¹), and KHCO₃ (4.5 g L⁻¹) was selected as the feedstock used for CH₄ production. The seed sludge was collected from a mesophilic continuous anaerobic digester of a municipal wastewater treatment plant in northern Japan, stabilized in synthetic wastewater at 37 °C with rotary shaking at 120 rpm for 30 d and adjusted to 5 g volatile suspended solids (VSS) L⁻¹ before use.

Two types of enrichments pre-acclimated to high NH₄⁺ (5 g NH₄-N L⁻¹) and NaCl (30 g L⁻¹) concentrations served as the bioaugmentation inocula. These concentrations were selected based on their previously reported inhibitory concentrations in AD systems (Duc et al., 2022). Both enrichments were generated from mesophilic AD sludge in a municipal wastewater treatment plant in southern Japan through cultivation in the same synthetic wastewater for over six months with stepwise increments of NH₄⁺ and NaCl concentrations to the final level. Repeated-batch mode was adopted for cultivation, with a batch time of 10 d. The CH₄ production activity of both enrichment systems was confirmed prior to the experiment; the results and the characteristics of the enrichments used as bioaugmentation inoculum have been provided (see [supplementary material](#)). The specific microbial compositions of both enrichments are shown in [Figs. 4 and 5](#).

2.2. Repeated batch anaerobic digestion experiment

The AD reactors were operated in repeated-batch mode with total and working volumes of 117 and 40 mL, respectively. Mesophilic temperature (37 °C) and rotary shaking (120 rpm) were maintained throughout the operation. The selected inhibition conditions were consistent with the pre-acclimated enrichments (ammonia inhibition: 5 g of NH₄-N L⁻¹; salt inhibition: 30 g NaCl L⁻¹). Anaerobic conditions were maintained by sealing the serum bottles with a butyl rubber stopper and flushing N₂ gas for 8 min. Five experimental groups were established in duplicate for ammonia- and salt-inhibited conditions: (1) 2.5 I: one-time introduction of 2.5 % (VSS base, the same below) bioaugmentation inoculum in the first batch; (2) 2.5 RB: repeated introduction of 2.5 % bioaugmentation inoculum in all three batches, making total dosage reach 7.5 %; (3) 5 I: one-time introduction of 5 % bioaugmentation inoculum in the first batch; (4) 7.5 I: one-time introduction of 7.5 % bioaugmentation inoculum in the first batch; (5) 5 II: one-time introduction of 5 % bioaugmentation inoculum in the second batch. The Control group (without inhibition or bioaugmentation) and the Inhibited group (inhibition without bioaugmentation inoculum), were also prepared in duplicate. Three consecutive batches of 81 d (27 d per batch) were conducted. CH₄ production was monitored every 2–3 d. Liquid samples were collected on days 8, 15, and 27 from each batch for VFAs measurements. The pH, ammonium/salt concentration, and soluble chemical oxygen demand (sCOD) of the liquid samples were measured, and biomass samples were collected at the end of each batch. When starting the next batch, the bulk liquid in each group was centrifuged under anaerobic conditions, the supernatant was discarded, and feedstock (together with bioaugmentation inoculum, if applicable) was replenished to the working volume. N₂ flushing was repeated before the reactors were placed in an incubator.

2.3. Chemical analytical method

Total suspended solids, VSS, CH₄ gas, sCOD, VFAs, NH₄⁺ and Na⁺ were analyzed as previously described (Duc et al., 2022). The concentrations of VFAs were calculated as COD (mg L⁻¹) with conversion coefficients of 1.07, 1.51, 1.82, and 2.04 for acetate, propionate, butyrate, and valerate, respectively.

The modified Gompertz model (Eq. (1)) was used to describe the

cumulative CH₄ production in each batch test:

$$M = P * \exp\left\{-\exp\left[\frac{B * R' * e}{P}(\lambda - t) + 1\right]\right\} \quad (1)$$

where M is the cumulative CH₄ production (mL) during operation, t is the operation time (d), and λ is the lag-phase time (d); P is the CH₄ production potential (mL); B is the biomass contained in the serum bottle (g VSS); and R' is the maximal CH₄ producing rate (mL CH₄ g VSS⁻¹ d⁻¹). Kinetic parameters were estimated by nonlinear curve fitting using the solver tool in Microsoft Excel (version 16.70).

2.4. Microbial community analysis

The methods for DNA extraction and 16S rRNA gene amplicon sequencing were the same as those previously described (Duc et al., 2023). To predict the gene abundance of key enzymes in the microbial community, the total sequencing reads were analyzed using the phylogenetic investigation of communities by the reconstruction of unobserved states 2 (PICRUSt2) software (Caicedo et al., 2020) and annotated according to the Kyoto Encyclopedia of Genes and Genomes (KEGG) database. The abundant metabolic genes related to glycolysis, fatty acid synthesis, propionic and butyric acid degradation, and aceticlastic and hydrogenotrophic methanogenesis were selected based on the KEGG methane metabolic pathways (Map: 00010, Map: 00061, Map:00013, Map:00357, and Map:00567) and evaluated accordingly. The sequencing data have been deposited with links to BioProject accession number PRJDB18095 in the DNA Data Bank of Japan BioProject database.

2.5. Statistical analysis

GraphPad Prism (v. 10, GraphPad Software Inc., USA) was used to plot the parameters estimated by the modified Gompertz equation. Multiple comparisons of ordinary two-way analysis of variance (ANOVA) were selected for the significance analysis among different groups. A significance level of 0.05 was applied. Principal component analysis (PCA) using the plug-in unit of Principal Component Analysis App in OriginLab program (v. 9.8.0.200, OriginLab Corporation, USA) was conducted to compare the microbial communities in different experimental groups and to show the succession of the microbial community in one group.

3. Results and discussion

3.1. CH₄ production

The reactor performance and kinetic parameters estimated using the modified Gompertz equation for each group are presented in Fig. 1 and the supplementary material. Bioaugmentation at all dosages exerted an instant mitigating effect in the first batch compared with the Inhibited groups in the ammonia- and salt-inhibited experiments. For example, the final cumulative CH₄ production in the 7.5 I group was 1.43-fold and 1.55-fold higher than their respective Inhibited group under ammonium and salt stress. Moreover, the mitigation performance was positively correlated with the dosage of the introduced inoculum for both inhibitors. The P values (see supplementary material) estimated by the modified Gompertz equation for the 2.5 I (87.5 %, compared with the Control group), 5 I (91.4 %), and 7.5 I (97.1 %) groups increased as the dosage increased under salt-inhibited conditions. The same trend was observed under ammonium stress, as P values increased from 85.5 % in the 2.5 I group to 96.5 % and 100.0 % in the 5 I and 7.5 I groups, respectively, with the increase in dosage. These results also conform to those of previous studies by Linsong et al. (2022) and Yang et al. (2016). However, the positive correlation between reactor performance and bioaugmentation inoculum dosage did not persist for either inhibitor. More specifically, in the salt-inhibited condition, the CH₄ production curves of the 2.5 I, 5 I, and 7.5 I groups in Fig. 1b overlapped in the second and third batches, indicating no evident difference in bioaugmentation efficiency among different dosage groups. The quantitative results were verified (see supplementary material and Fig. 2) as the P values of the aforementioned three groups and the 2.5 RB and 5 II groups in the salt-inhibited experiment did not exhibit significant differences ($p > 0.05$) in the third batches by multiple comparisons. This suggests that all bioaugmented groups performed similar mitigating effects regardless of the bioaugmentation regimes after stabilization under salt stress.

For the ammonia-inhibited condition, a distinct difference from the salt-inhibited experiment was observed in the 2.5 I group. In both the second and third batches, the 2.5 I group exhibited significantly better mitigating performance ($p < 0.05$), with final cumulative CH₄ production that was 12 % and 10 % higher than in the 7.5 I group in the second and third batches, respectively. This reversed the positively correlated relationship between the dosages and mitigating performances observed in the first batch. Excluding the 2.5 I group, the remaining bioaugmented groups exhibited no significant difference ($p > 0.05$) in

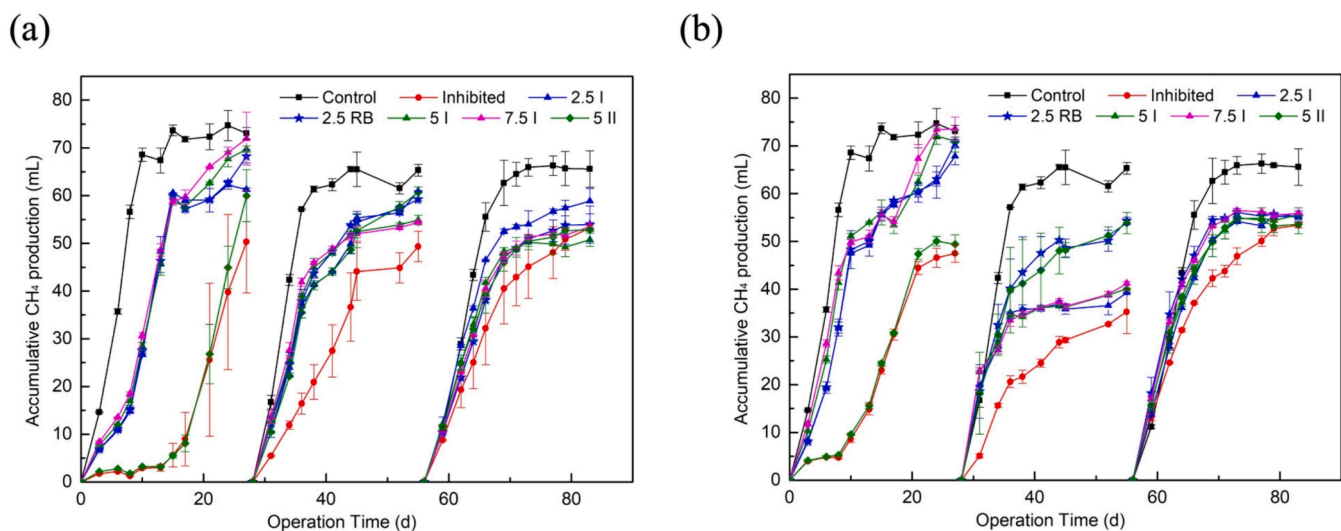


Fig. 1. Methane production profile in repeated batches of the (a) ammonia- and (b) salt-inhibited experiments. The error bars represent the standard deviation of the mean for each duplicate experiment.

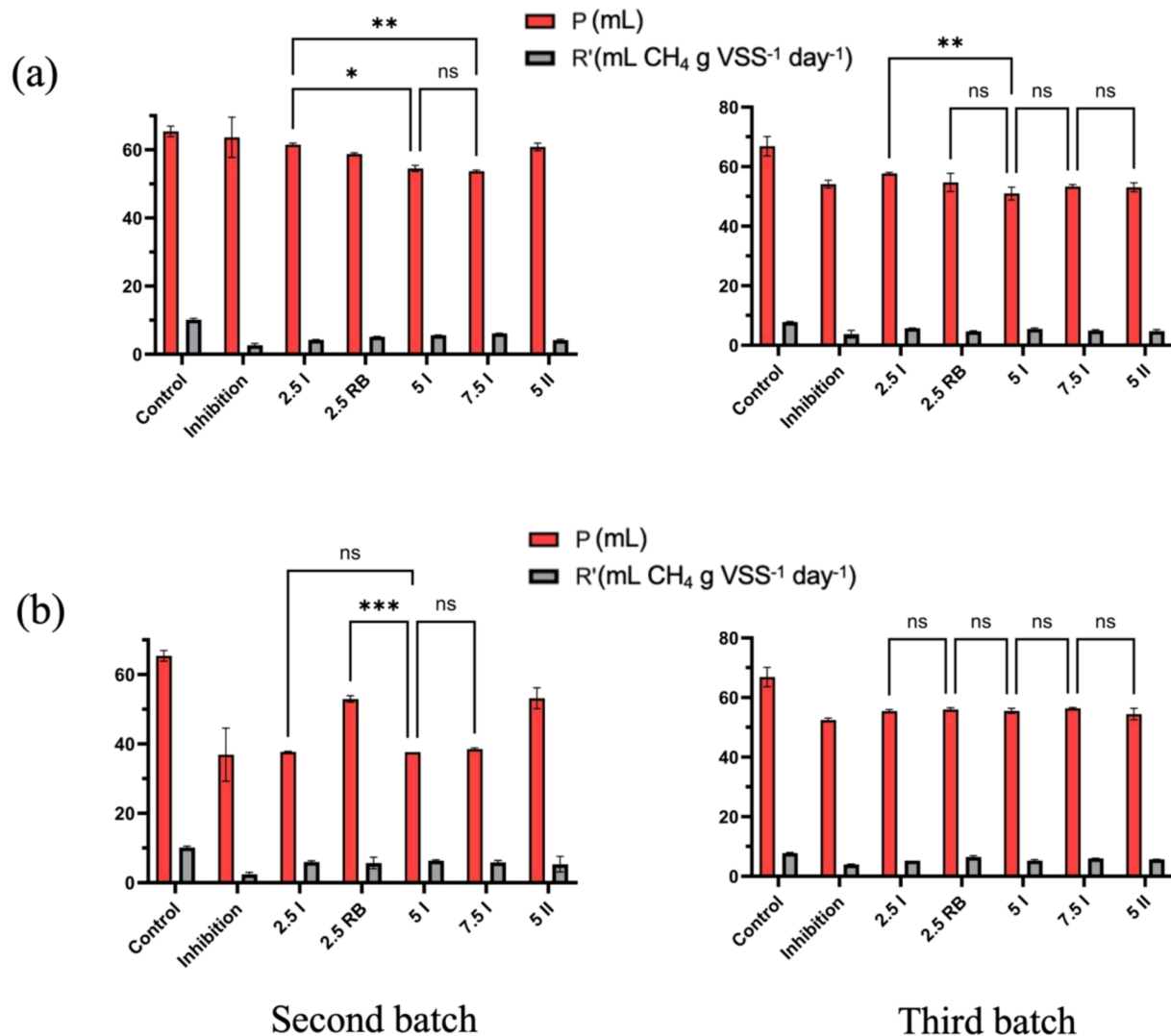


Fig. 2. Parameters estimated using the modified Gompertz equation in the second and third batches of the (a) ammonia- and (b) salt-inhibited experiments. Solid lines indicate significant differences between groups (* $p < 0.05$; ** $p < 0.01$; *** $p < 0.001$; ns: not significant). The error bars represent the standard deviation of the mean for each duplicate experiment.

performance in the third batch, indicating that the stabilized performance of the bioaugmented groups also partly applied to the ammonia-inhibited condition. In addition, for both inhibitors, the P values of the Inhibited groups in the second and third batches exhibited no significant difference ($p > 0.05$) with one or more bioaugmented groups. This was due to the enhanced CH₄ production activity in the Inhibited groups, potentially caused by the relatively long acclimation time.

Collectively, these results indicate the temporality of the positive correlation between reactor performance and bioaugmentation inoculum dosages, as well as a converging trend for the different bioaugmented groups as the operation progressed under both inhibited conditions.

The effect of repetition was evaluated by comparing the performance of the 2.5 RB group to the group with the same overall dosage at that time (i.e., 5 I and 7.5 I groups in the second and third batches, respectively). In the salt-inhibited condition, the P value in the 2.5 RB group was 1.38-fold higher than that in 5 I group, whereas the ratio decreased to 0.99-fold that of the 7.5 I group in the third batch (see [supplementary material](#)). A similar trend was observed under ammonia-inhibited conditions. Hence, the advantageous effects of repetition weakened as the number of batches increased.

When considering the repeated introduction of a 2.5 % inoculum as a

separate event in each batch, a diminishing marginal effect could be intuitively perceived as the level of performance enhancement decreased with increasing batch number. Eventually, no distinguishable enhancement in performance was achieved by the newly introduced inoculum, with no significant difference ($p > 0.05$) in performance was observed between the 2.5 RB group and other bioaugmented groups (Fig. 2) in the third batch of either inhibited condition. These results contradict the findings of Yang et al. (2016), who claimed that the repeated bioaugmentation continued to outcompete one-time bioaugmentation. More specifically, Yang et al. (2016) employed propionate-degrading paddy soil enrichments incubated with various individual VFAs mixtures to accelerate the utilization of VFAs in anaerobic systems with an every-time dosage of 0.045 g VS/L. This discrepancy may be attributed to their short batch time (15 d for each batch) in Yang et al. (2016), as 45 d may not be sufficient to observe decrease in performance of the repeated bioaugmentation group.

The effect of timing was also evaluated by comparing the performances of the 5 I, 5 II, and Inhibited groups. Both 5 I and 5 II groups substantially improved CH₄ production after bioaugmentation. Hence, bioaugmentation inoculum could exert its mitigating effect by simultaneous or delayed introduction of the inhibitors, which agrees with previous reports (Cai et al., 2021; Li et al., 2017). However, for both

inhibited conditions, the convergence occurred as the operation progressed in the 5 I and 5 II groups, regardless of the bioaugmentation timing.

3.2. Volatile fatty acids accumulation

VFAs, including acetate, propionate, butyrate, and valerate, are important intermediates in the AD process as they connect soluble organic monomers to the final methanogenic phase and are often used to evaluate the performance of AD processes. Given that the utilization of VFAs is thermodynamically unfavorable (Mao et al., 2015), with aceticlastic methanogens vulnerable to various inhibitors, VFAs accumulation is often observed in problematic AD systems.

The total VFAs concentration profiles during the AD experiments are shown in Fig. 3a and c. In the salt-inhibited experiment, the accumulation of total VFAs in the first batch was markedly higher than in the subsequent batches, with the maximum concentration of the Inhibited group exceeding 4000 mg COD L⁻¹. This may be attributed to the stalled status of VFAs conversion, as relatively low CH₄ production was observed in the first 8 days in the first batch (Fig. 1). In the ammonia-inhibited experiment, the accumulation of total VFAs exceeded 4500 mg COD L⁻¹, and lagged accumulation peaks were observed on day 15 in the first and second batches of the Inhibited and 5 II groups, indicating more severely inhibited methanogenesis processes. This was also supported by the extended lag-phase time (λ) estimated using the modified Gompertz equation (see supplementary material), compared with the salt-inhibited experiment. This discrepancy may be due to the different inhibition mechanisms of ammonia and salt. Salt overdosing alters the osmotic pressure in the cell, leading to cell disintegration and reduced

metabolic enzyme activity in CH₄ production (Wood, 2015). Similarly, ammonia overdosing also impacts the osmotic pressure; however, free ammonia and NH₄⁺ inhibit methanogenesis by competing with enzymatic reactions for intracellular protons and interfering with interactions at the Ca²⁺ and Mg²⁺ sites of enzymes participating in CH₄ synthesis, respectively (Li et al., 2023). Moreover, propionate accumulation was observed in both Inhibited groups at the end of the first batch. This agrees with the results of Duc et al. (2022), who claimed that propionate is a deterministic factor affecting CH₄ production and is prone to accumulation under ammonium and salt inhibition. However, in the subsequent batches of both inhibitor experiments, the proportion of propionate in the accumulated VFAs sharply decreased in most experimental groups. Further investigation is needed to explain whether this is due to an enhanced propionate-utilizing ability or deteriorated production.

Evaluation of the overall system status when deterioration occurs provides insights into the cause(s) of the observed performance convergence. As shown in Fig. 1, four common deteriorations in performance were observed for both inhibitors: (1) the 5 I group in the second batch, (2) the 7.5 I group in the second batch, (3) the 2.5 RB group in the third batch, and (4) the 5 II group in the third batch. Regarding the deterioration of the 2.5 RB group in the third batch, an increased VFAs concentration was observed compared with that in the second batch of both inhibitors (Fig. 3 and see supplementary material). In the ammonia-inhibited experiment, the final accumulated VFAs concentration increased from 156.8 mg COD L⁻¹ in the second batch to 291.0 mg COD L⁻¹ in the third batch. This suggests that the weakened ability to utilize VFAs resulted in the deterioration of the 2.5 RB group. For the 5 I and 7.5 I groups, the final sCOD concentrations in the second

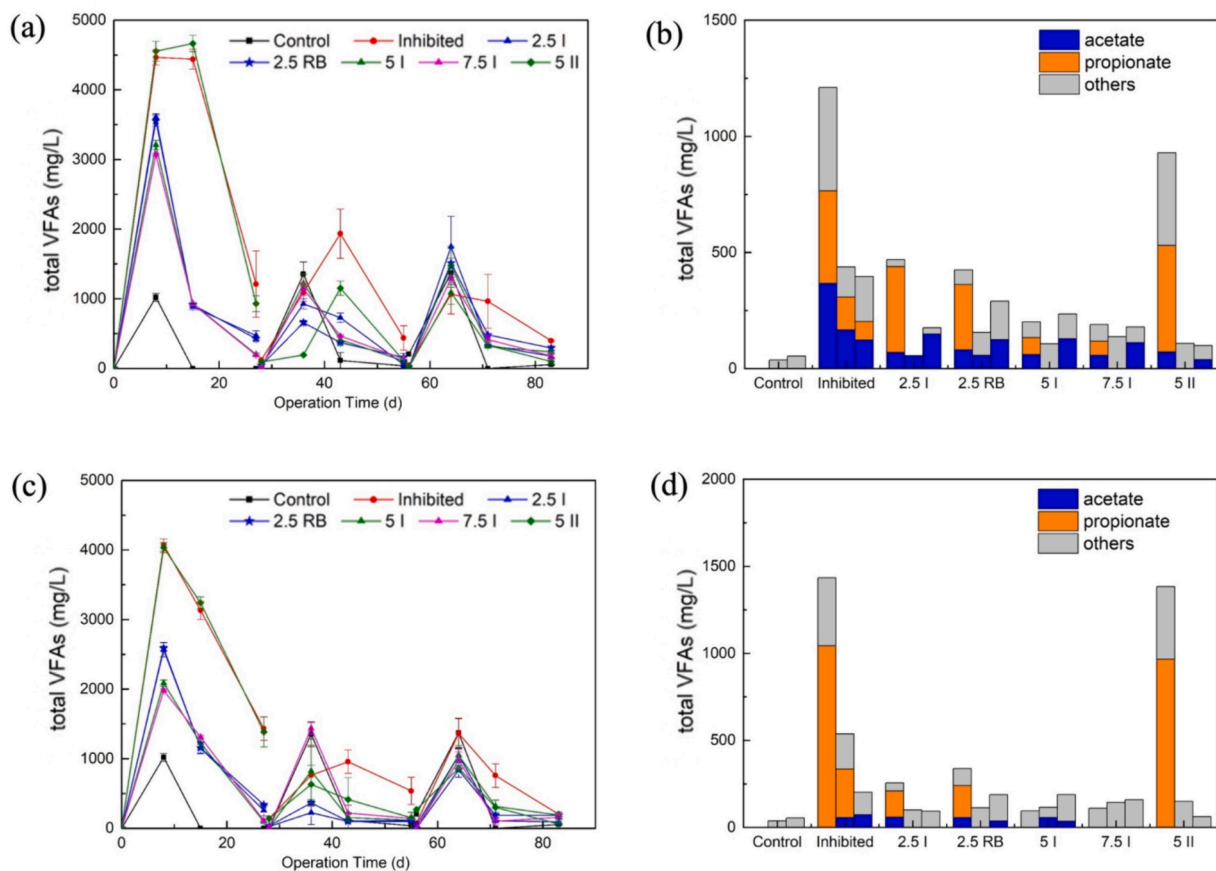


Fig. 3. Total volatile fatty acids (VFAs) concentration profile in repeated batches of the (a) ammonia- and (c) salt-inhibited experiments. Accumulated concentrations of different VFAs at the end of each batch of the (b) ammonia- and (d) salt-inhibited experiments. The three bars in the same cluster represent the results of, from left to right, the first, second, and third batches. The error bars represent the standard deviation of the mean for each duplicate experiment.

batch were higher than those in the first batches for both inhibitors. For example, the sCOD concentration of the 5 I group in the ammonia-inhibited experiment increased from 1662.5 mg COD L⁻¹ to 3187.5 mg COD L⁻¹ in the second batch. This suggests that the issue may stem from hydrolysis and acidogenesis, supported by actual VFAs production data on day 8 calculated by adding the COD equivalents of the total VFAs and CH₄ produced (see [supplementary material](#)), according to Li et al. (2015). The actual VFAs production on day 8 in the second batch was lower than that in the first batch in these two groups of both inhibitors. For example, the actual VFAs production of the 7.5 I group in the salt-inhibited experiment decreased from 5085.4 mg COD L⁻¹ in the first batch to 3826.8 mg COD L⁻¹ in the second batch, indicating weakened VFAs production. Despite the relatively high tolerance of acidogenic bacteria to inhibitors compared with that of methanogens (Li et al., 2022), their abundance and activity can be influenced by other changes in ambient parameters, such as the exotic microorganisms from bioaugmentation. The deterioration of the 5 II group in the third batch

did not adhere to either of the two defined patterns and, thus remained unexplained using the VFAs data.

3.3. Microbial community succession

3.3.1. Archaeal community

The archaeal community succession of each experimental group in the ammonia- and salt-inhibited experiments is shown in Fig. 4a and b, respectively. The dominant genus in the seed sludge was *Methanosaeta*, a typical aceticlastic methanogen vulnerable to ammonium and salt inhibition (Yan et al., 2019; Zhang et al., 2016). For the pre-acclimated enrichments used as bioaugmentation inocula for both inhibitors, the most abundant genus was *Methanosarcina*, a facultative methanogen known to perform both aceticlastic and hydrogenotrophic pathways (Tian et al., 2018), followed by the hydrogenotrophic methanogens *Methanobacterium* and *Methanoculleus*. All experimental groups, excluding the Control group, experienced considerable archaeal

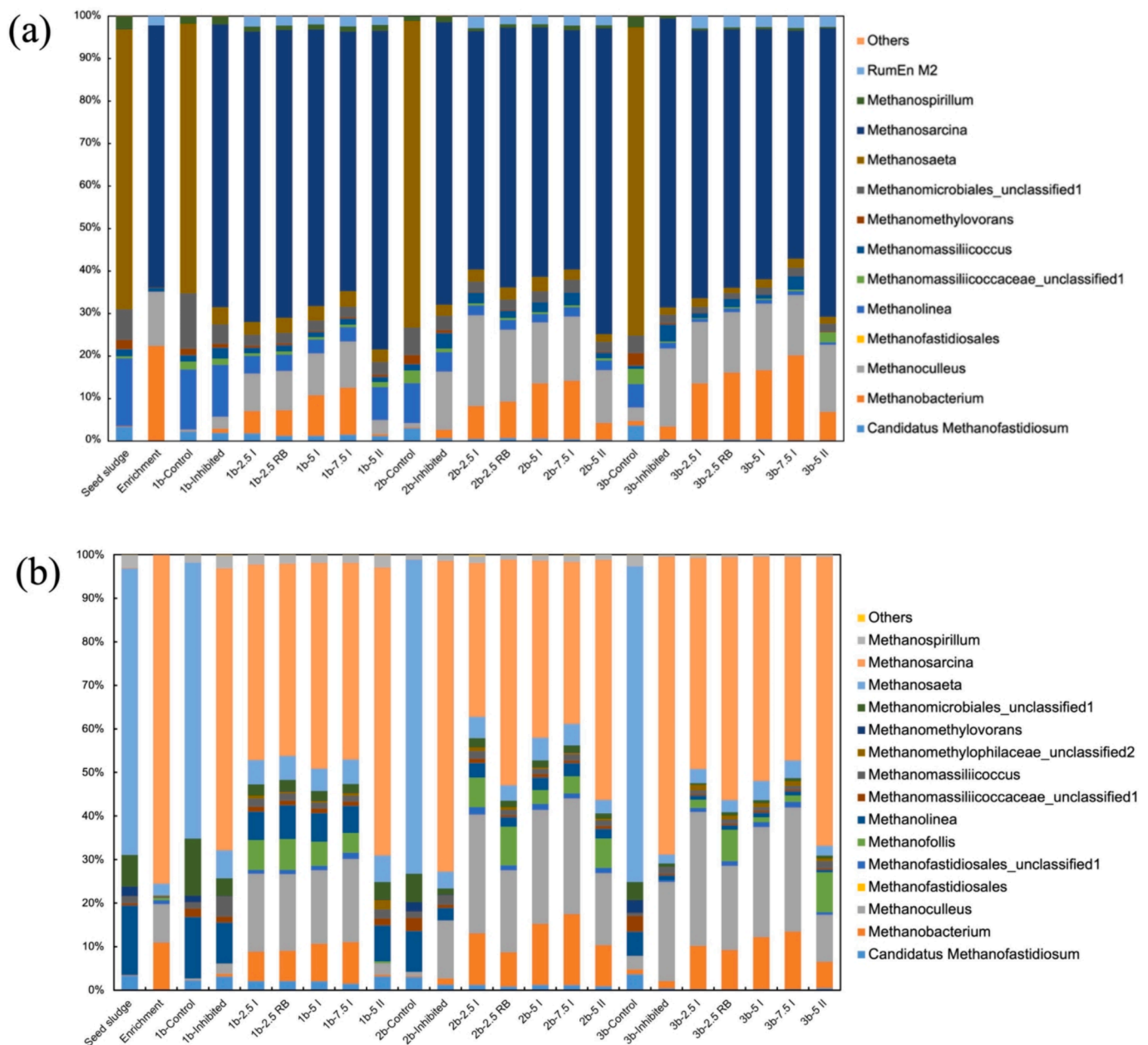


Fig. 4. Relative abundance of archaeal communities in repeated batches of the (a) ammonia- and (b) salt-inhibited experiments at the genus level. Genera under 1% relative abundance were allocated to “Others.” “b” in the sample names stands for “batch.”

community changes at the end of the first batch compared to the seed sludge for both inhibitors (Fig. 4). Hence, bioaugmentation and the inhibiting conditions markedly impacted the composition of the archaeal community. *Methanosarcina* dominated in all bioaugmented groups (over 60 % and 40 % in the ammonium and salt-inhibited experiments, respectively), replacing *Methanosaeta*, regardless of the inhibitor type. At the end of the first batch, the abundance of *Methanobacterium* was positively correlated with bioaugmentation dosage but remained unchanged in the Inhibited groups for both inhibitors. For example, the abundance increased from 0.42 % in the seed sludge to 5.27 % (2.5 I group), 9.52 % (5 I group), and 11.02 % (7.5 I group) in the ammonia-inhibited experiment. This suggests that the abundance of *Methanobacterium* can be regarded as an indicator of bioaugmentation contribution. In contrast, the abundance of *Methanoculleus* increased irrespective of the bioaugmented and Inhibited

groups, which may be attributed to the superior resilience of *Methanoculleus* compared to other methanogens (Capson-Tojo et al., 2020).

Within the bioaugmented groups in both inhibiting experiments, the structure of the archaeal communities rapidly corresponded to their respective pre-acclimated enrichments at the end of the first batch. *Methanosarcina*, *Methanoculleus*, and *Methanobacterium* became the most abundant genera in all bioaugmented groups as in the enrichment groups, and their predominance was sustained during further operation. In the salt-inhibited experiment, the relative abundance of *Methanosarcina* in the bioaugmented groups declined by ca. 10 %, excluding a 5 % increase in the 2.5 RB group at the end of the second batch, potentially responsible for the superior performance of the 2.5 RB group. However, despite another 5 % increase in the *Methanosarcina* abundance at the end of the third batch, the performance of the 2.5 RB group converged with other bioaugmented groups. Additionally, a relatively

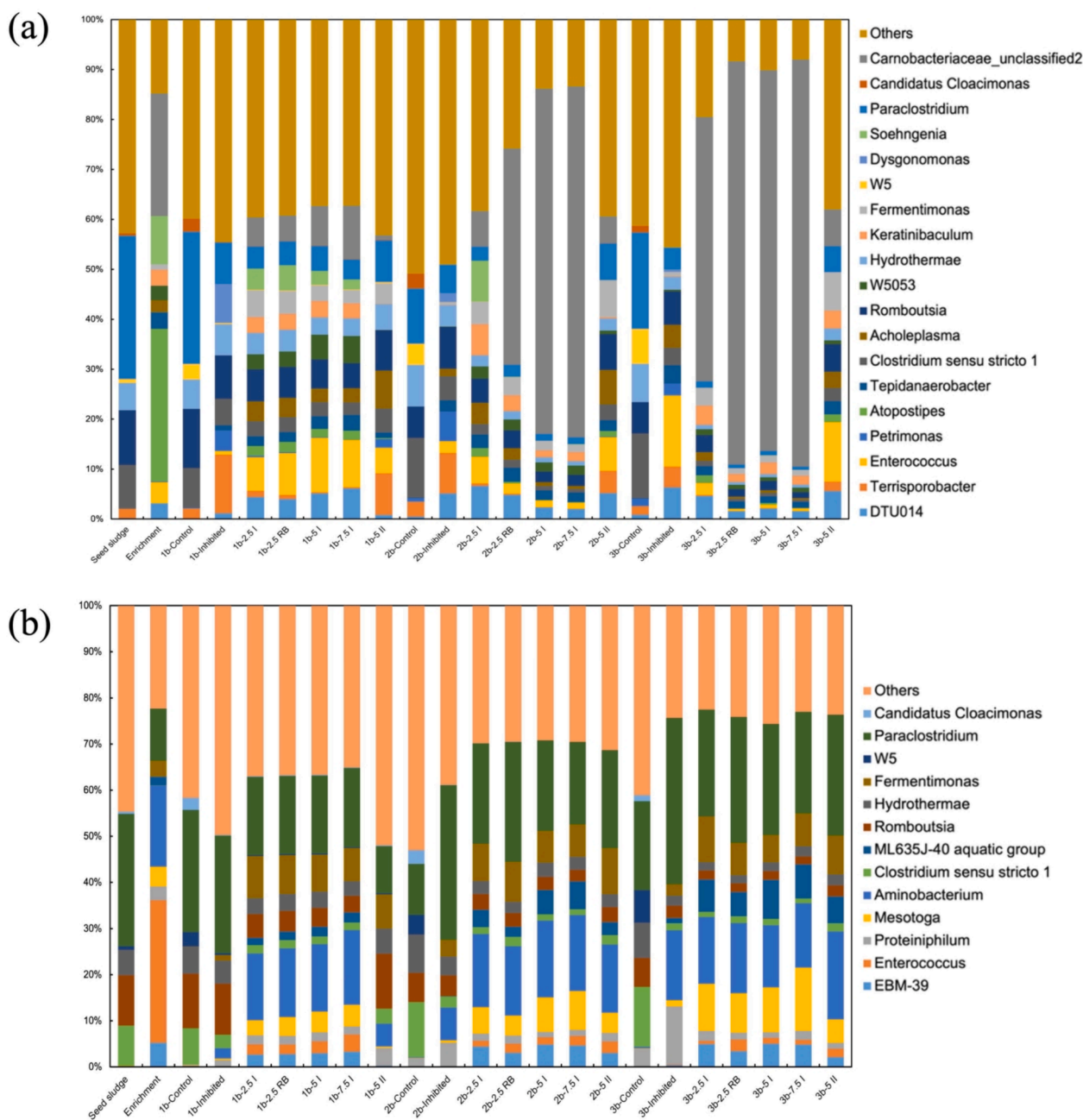


Fig. 5. Relative abundance of bacterial communities in repeated batches of the (a) ammonia- and (b) salt-inhibited experiments at the genus level. Genera under 5% relative abundance were allocated to “Others.” “b” in the sample names stands for “batch.”

distinct structure of the archaeal community arose in the 5 II group throughout the operation, with an even higher *Methanosarcina* abundance (over 65 %), which did not prevent performance convergence in the third batch. Moreover, despite the exceptional performance of the 2.5 I group, the *Methanosarcina* abundance did not differ from the 5 I and 7.5 I groups in the ammonia-inhibited experiment. In addition, the abundance of *Methanobacterium* was positively correlated with the bioaugmentation dosages throughout the experiment, whereas the performance was completely reversed after the end of the first batch. In summary, the archaeal community was not the primary influencing factor in CH₄ production performance.

3.3.2. Bacterial community

Bacteria play a major role in the hydrolysis, acidogenic, and acetogenic stages of the AD system (Wang et al., 2023), thus displaying a more complicated community structure than archaea. The succession of the bacterial communities in each experimental group in the ammonia- and salt-inhibited experiments is shown in Fig. 5a and b, respectively. The dominant bacteria in the seed sludge were *Paraclostridium* (28.7 %), *Romboutsia* (10.9 %), and *Clostridium sensu stricto 1* (8.7 %). For the enrichment pre-acclimated to ammonia, the dominant bacteria were *Atopostipes* (30.5 %), *Carnobacteriaceae_unclassified2* (24.6 %), and *Soehngenia* (9.7 %). Regarding salt enrichment, *Enterococcus* (30.9 %), *Aminobacterium* (17.6 %), and *Paraclostridium* (11.3 %) were the dominant genera. Most of these bacteria are capable of mediating processes such as fermentation (Cai et al., 2021), acid production (Khafipour et al., 2020), and acid oxidation (Wang et al., 2019). The diverse dominant bacteria in the different enrichments can attribute to the functional diversity and redundancy of the bacterial community (Zhang et al., 2022). In contrast to archaea, a limited number of bacteria were strengthened by bioaugmentation inoculum for both inhibitors (e.g., *Carnobacteriaceae_unclassified2* in the ammonia-inhibited experiment and *Aminobacterium* in the salt-inhibited experiment). The succession patterns of the bacterial community in the ammonia- and salt-inhibited experiments were also distinct, providing additional insights regarding how the bacterial community influences the reactor performance.

In the ammonia-inhibited experiment, balanced and diversified bacterial communities were formed for all bioaugmented groups at the end of the first batch, with the most dominant genus constituting ca. 10 % abundance (Fig. 5a) and the Shannon index peaking at ca. 4.5 (see supplementary material). However, at the end of the second batch, this balance was disrupted by an abrupt increase in *Carnobacteriaceae_unclassified2* abundance to 69.1 % and 70.3 %, along with decreased Shannon indexes to 2.12 and 2.06 for the 5 I and 7.5 I groups, respectively. Although *Carnobacteriaceae_unclassified2* is reportedly involved in the degradation of polysaccharides and sugars (Banti et al., 2023), other biochemical processes can be weakened by an overly homogeneous bacterial community. Thus, it is postulated that the deteriorations in the performance of the 5 I, 7.5 I, and 2.5 RB groups, were related to the marked changes in the bacterial community as the relative abundance of *Carnobacteriaceae_unclassified2* in the 2.5 RB group also increased to a comparable value (80.7 %) at the end of the third batch. In contrast, regarding the exceptional CH₄ production performance of the 2.5 I group, the relative abundance of *Carnobacteriaceae_unclassified2* increased relatively slowly (7.2 % and 52.9 % at the end of the second and third batches, respectively), presumably due to having the lowest bioaugmentation dosage. The abundance of *Carnobacteriaceae_unclassified2* in the 5 II group exhibited minimal differences as the operation progressed. Moreover, the overall structure of the bacterial community in the 5 II group was dissimilar from the other bioaugmented groups; this may be attributed to the altered interactions among bacteria caused by the delayed bioaugmentation. Evidence supporting these proposals based on VFAs data can also be found in the microbial succession process. For the enhanced accumulation of VFAs in the 2.5 RB group in the third batch, the decreased abundance of the acid-oxidizing bacteria such as *Acholeplasma* (Li et al., 2015) and *Tepidanaerobacter*

(Wang et al., 2023) was confirmed. Additionally, The abundance of acid-producing *Enterococcus* (Woraruthai et al., 2024) decreased sharply from 10.88 % to 1.32 % in the 5 I group and from 9.50 % to 1.20 % in the 7.5 I group, as weakened VFAs production ability was suspected to be the cause of the deterioration occurred in the 5 I and 7.5 I groups in the second batch.

Similar performance deterioration was observed in the salt-inhibited experiment in the absence of marked changes in subsequent succession, as in the ammonia-inhibited experiment. Evidence supporting these proposals based on VFAs data can also be found as the decreased abundance of the acid-oxidizing *Fermentimonas* (Ziganshina and Ziganshin, 2022) was observed in the 2.5 RB group, together with the decreased abundance of acid-producing bacteria such as *Enterococcus* and *Romboutsia* (Castro-Ramos et al., 2022) was observed in the 5 I and 7.5 I groups. In addition, unlike in the ammonia-inhibited experiment, the bacterial structure of the 5 II group converged with that of the other bioaugmented groups at the end of the third batch. This may be attributed to the relatively mild inhibition of the salt-inhibited condition. Hence, the changes in performance among experimental groups can be explained by the succession of bacterial communities, which also supports proposals based on VFAs data.

3.4. Functional prediction based on 16S rRNA amplicon sequencing

To obtain a more comprehensive understanding of the potential functional changes that occurred during operation, the PICRUSt2 method was used to predict the relative abundances of key enzymes related to AD. Eleven, nine, and ten enzyme-encoding genes related to acidogenesis, acetogenesis, and methanogenesis in the AD process were selected, respectively, based on their high relative abundances (Fig. 6). Acidogenesis was further subdivided into glycolysis and fatty acid biosynthesis pathways. Similarly, acetogenesis was subdivided into propionic acid and butyric acid degradation pathways, and methanogenesis was subdivided into acetoclastic and hydrogenotrophic methanogenesis pathways.

In the ammonia-inhibited experiment, the abundances of key enzymes for all three steps in the 5 I and 7.5 I groups showed synchronous changes in each batch. In the acidogenesis step, 2-oxoacid oxidoreductase (EC:1.2.7.11), which oxidatively decarboxylates pyruvate to acetyl-CoA (Zhao et al., 2023), was the most abundant enzyme-encoding gene constituting 68.78‰ and 65.61‰ in the 5 I and 7.5 I groups, respectively, at the end of the first batch. However, its relative abundance decreased sharply to 21.90‰ and 21.41‰ at the end of the second batch, respectively. With acetyl-CoA being the important precursor for acetate generation (Zhao et al., 2023), this sharp decline substantially limited the production of the direct substrate for CH₄ generation, impairing the entire AD process. Additionally, the relative abundance of long-chain fatty acid-CoA ligase (EC:6.2.1.3), which contributes to the elongation of various long-chain fatty acids, decreased sharply to approximately 0.35-fold in the 5 I and 7.5 I groups at the end of the second batch compared with that in the first batch. In addition to acidogenesis, a decreasing trend was also observed in key enzyme abundance associated with the acetogenesis and methanogenesis steps in the 5 I and 7.5 I groups. For example, the relative abundances of enoyl-CoA hydratase (EC:4.2.1.17) and methylmalonyl-CoA mutase (EC:5.4.99.2), which are involved in the propionic and butyric acid degradation pathways, respectively (Wang et al., 2023), in the acetogenesis step and tetrahydromethanopterin S-methyltransferase (EC:2.1.1.86), which is involved in a crucial step transferring the methyl group from CH₃-H₄MPT to methyl-CoM (Liu et al., 2021) in the methanogenesis step, decreased to less than 0.5-fold at the end of the second batch compared with that in the first batch in the 5 I and 7.5 I groups. It is worth noticing that decreases in the abundance of these enzymes can not only result in the impaired CH₄ production, but also can aggregate the accumulation of VFAs, creating even inhibitory conditions for microbial growth.

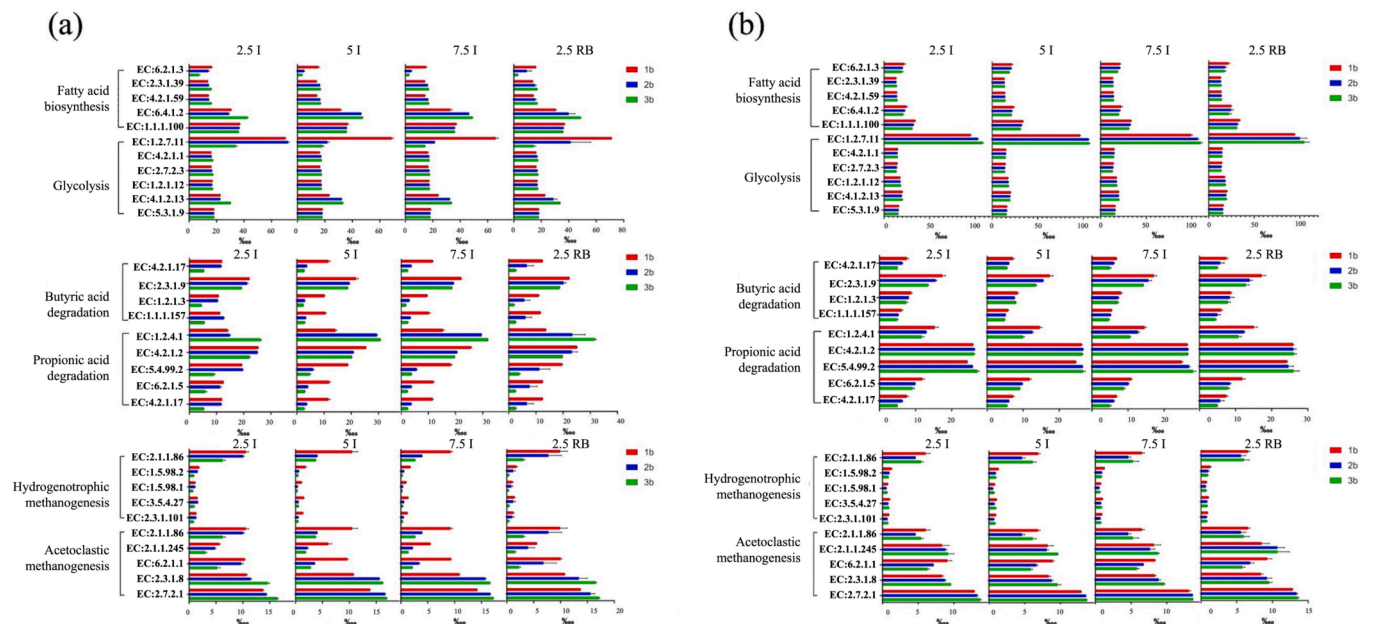


Fig. 6. Predicted relative abundances of key enzymes related to acidogenesis, acetogenesis, and methanogenesis in anaerobic digestion with (a) ammonia and (b) salt inhibition using the PICRUST2 method. The error bars represent the standard deviation of the mean for each duplicate experiment.

Collectively, these results indicated that an overall decline in all three steps occurred in the 5 I and 7.5 I groups at the end of the second batch. In contrast, the relative abundance of numerous key enzymes was sustained throughout the experiment in the 2.5 I group, which might contribute to its exceptional CH₄ production. In the salt-inhibited experiment, the discrepancies in relative abundance among different batches and different groups were markedly smaller than those in the ammonia-inhibited experiment. Nevertheless, a slight decrease in the relative abundance of numerous key enzyme genes was observed in all three steps. More specifically, a decreased relative abundance of acetyl-CoA carboxylase (EC:6.4.1.2), which forms carbon-carbon bonds in VFAs biosynthesis, was observed in the 5 I and 7.5 I groups, and a decreased relative abundance of pyruvate dehydrogenase (acetyl-transferring) (EC:1.2.4.1), which participates in the propionic acid degradation pathway in the acetogenesis step, was observed in 2.5 RB group.

In summary, functional prediction based on 16S rRNA amplicon sequencing data suggested an overall decline in all three steps of the AD process in most experimental groups, regardless of the inhibitor, resulting in converged and deteriorated performance for groups with different bioaugmentation regimes.

3.5. Steady state for bioaugmentation

Despite the temporary CH₄ production performance divergence in the first batch, the discrepancy among the bioaugmented groups diminished as the microbial community succession reached a steady state (Fig. 1). This was also supported by the PCA results (see [supplementary material](#)). The relative distances between groups with different bioaugmentation regimes in archaeal and bacterial communities decreased as the number of batches increased, regardless of the inhibitor, indicating a converging trend for the microbial communities. Corroborating evidence regarding the CH₄ production profile and VFAs accumulation suggests that the deteriorated performance in different bioaugmented groups may be due to the weakened VFAs production and VFAs utilizing abilities. While taking together the microbial analysis results, both reasons stem from the less diversified bacterial community, which resulted in the overall decline in different steps in AD process. It can be speculated that the groups with higher inoculum doses promptly

reached a steady state. The small dosage introduced to the 2.5 I group in the ammonia-inhibited experiment slowed the succession process, rendering exceptional CH₄ production performance. For repetitive introduction, the more the microbial community approached a steady-state structure, the smaller the role the bioaugmentation inoculum had in shaping the microbial community. Regarding the timing of bioaugmentation, it can be speculated that the markedly altered microbial community after the first batch caused the discrepancy in converging results for the 5 II groups of the different inhibitors, as the final steady state was shaped by cooperative interactions between the inhibiting conditions, seed sludge, and bioaugmentation inoculum. As the results showed, the transition state performance in the first batch exceeded the performance in the final steady state in both inhibiting experiments. Thus, maintaining the transition state by periodically discharging the fermentation bulk liquid and introducing inoculum in continuous-mode reactors may be ideal for maintaining the mitigating effects of bioaugmentation in AD reactors. This proposal seems to contradict the conclusions of [Tian et al. \(2017\)](#), which claimed that, compared with batch and fed-batch reactors, a continuous reactor is unfavorable to sustain the slow-growing methanogens, as they might be washed out of the reactor. However, the washout effect in a continuous-mode reactor does not necessarily deteriorate the AD process. This was demonstrated by [Christou et al. \(2021\)](#) who realized a long-term increase in CH₄ production within continuous-mode AD reactors via one-time bioaugmentation. Moreover, bioaugmented reactors can even successfully resist the strengthened washout effect by shortening the hydraulic retention time. However, given that these studies are all restricted to bench-scale reactors, further large-scale applications are yet to be explored. An additional benefit of operating in continuous-mode is that the toxicant accumulation of byproducts is mitigated by the daily input and output of the bulk liquid, which may help maintain a suitable environment for the growth of various microorganisms ([Tian et al., 2017](#)).

4. Conclusions

This study revealed the temporality of the previously reported positive correlation between AD performance and bioaugmentation inoculum dosages. The microbial community in the bioaugmented groups

converged to a deteriorated steady state as the operation progressed. A homogeneous bacterial community with dominant *Carnobacteriaceae_unclassified2* caused the decline of CH₄ production in the ammonia-inhibited experiment. Hence, a balanced and diversified bacterial community is key for active CH₄ production. However, methods to achieve this condition have yet to be explored. One potential method includes maintaining the transition state by periodically discharging the fermentation bulk liquid and introducing inoculum in continuous-mode reactors.

Funding

This study was supported by the JPNP18016 project commissioned by the New Energy and Industrial Technology Development Organization (NEDO) of Japan. Zi-Yan Li would like to thank the China Scholarship Council for financial support.

CRediT authorship contribution statement

Zi-Yan Li: Writing – original draft, Methodology, Investigation, Formal analysis. **Shintaro Nagao:** Investigation, Formal analysis. **Daisuke Inoue:** Writing – review & editing, Supervision, Resources, Conceptualization. **Michihiko Ike:** Writing – review & editing, Supervision, Resources, Project administration, Funding acquisition, Conceptualization.

Declaration of competing interest

The authors declare that they have no known competing financial interests or personal relationships that could have appeared to influence the work reported in this paper.

Data availability

Data will be made available on request.

Appendix A. Supplementary data

Supplementary data to this article can be found online at <https://doi.org/10.1016/j.biortech.2024.131481>.

References

- Banti, D., Samaras, P., Chioti, A., Mitsopoulos, A., Tsangas, M., Zorpas, A., Sfetsas, T., 2023. Improvement of MBBR performance by the addition of 3D-printed biocarriers fabricated with 13X and bentonite. *Resources* 12, 81. <https://doi.org/10.3390/resources12070081>.
- Cai, G., Zhao, L., Wang, T., Lv, N., Li, J., Ning, J., Pan, X., Zhu, G., 2021. Variation of volatile fatty acid oxidation and methane production during the bioaugmentation of anaerobic digestion system: microbial community analysis revealing the influence of microbial interactions on metabolic pathways. *Sci. Total Environ.* 754, 142425 <https://doi.org/10.1016/j.scitotenv.2020.142425>.
- Caicedo, H.H., Hashimoto, D.A., Caicedo, J.C., Pentland, A., Pisano, G.P., 2020. Overcoming barriers to early disease intervention. *Nat. Biotechnol.* 38, 669–673. <https://doi.org/10.1038/s41587-020-0550-z>.
- Capson-Tojo, G., Moscoviz, R., Astals, S., Robles, Á., Steyer, J.-P., 2020. Unraveling the literature chaos around free ammonia inhibition in anaerobic digestion. *Renew. Sustain. Energy Rev.* 117, 109487 <https://doi.org/10.1016/j.rser.2019.109487>.
- Castro-Ramos, J.J., Solís-Oba, A., Solís-Oba, M., Calderón-Vázquez, C.L., Higuera-Rubio, J.M., Castro-Rivera, R., 2022. Effect of the initial pH on the anaerobic digestion process of dairy cattle manure. *AMB Express* 12, 162. <https://doi.org/10.1186/s13568-022-01486-8>.
- Chen, Y., Cheng, J.J., Creamer, K.S., 2008. Inhibition of anaerobic digestion process: a review. *Bioresour. Technol.* 99, 4044–4064. <https://doi.org/10.1016/j.biortech.2007.01.057>.
- Christou, M.L., Vasileiadis, S., Karpouzias, D.G., Angelidaki, I., Kotsopoulos, T.A., 2021. Effects of organic loading rate and hydraulic retention time on bioaugmentation performance to tackle ammonia inhibition in anaerobic digestion. *Bioresour. Technol.* 334, 125246 <https://doi.org/10.1016/j.biortech.2021.125246>.
- Duan, H., He, P., Zhang, H., Shao, L., Lü, F., 2022. Metabolic regulation of mesophilic *Methanosarcina barkeri* to ammonium inhibition. *Environ. Sci. Technol.* 56, 8897–8907. <https://doi.org/10.1021/acs.est.2c01212>.
- Duc, L.V., Miyagawa, Y., Inoue, D., Ike, M., 2022. Identification of key steps and associated microbial populations for efficient anaerobic digestion under high ammonium or salinity conditions. *Bioresour. Technol.* 360, 127571 <https://doi.org/10.1016/j.biortech.2022.127571>.
- Duc, L.V., Nagao, S., Mojarrad, M., Miyagawa, Y., Li, Z.-Y., Inoue, D., Tajima, T., Ike, M., 2023. Bioaugmentation with marine sediment-derived microbial consortia in mesophilic anaerobic digestion for enhancing methane production under ammonium or salinity stress. *Bioresour. Technol.* 376, 128853 <https://doi.org/10.1016/j.biortech.2023.128853>.
- Fan, Y., Yang, X., Lei, Z., Zhang, Z., Kobayashi, M., Adachi, Y., Shimizu, K., 2021. Alleviation of ammonia inhibition via nano-bubble water supplementation during anaerobic digestion of ammonia-rich swine manure: buffering capacity promotion and methane production enhancement. *Bioresour. Technol.* 333, 125131 <https://doi.org/10.1016/j.biortech.2021.125131>.
- Grady, C.P.L., Daigger, G.T., Lim, H.C., 1999. *Biological Wastewater Treatment*, second ed. Marcel Dekker, New York.
- Jo, Y., Rhee, C., Choi, H., Shin, J., Shin, S.G., Lee, C., 2021. Long-term effectiveness of bioaugmentation with rumen culture in continuous anaerobic digestion of food and vegetable wastes under feed composition fluctuations. *Bioresour. Technol.* 338, 125500 <https://doi.org/10.1016/j.biortech.2021.125500>.
- Khafipour, A., Jordaan, E.M., Flores-Orozco, D., Khafipour, E., Levin, D.B., Sparling, R., Cicek, N., 2020. Response of microbial community to induced failure of anaerobic digesters through overloading with propionic acid followed by process recovery. *Front. Bioeng. Biotechnol.* 8, 604838 <https://doi.org/10.3389/fbioe.2020.604838>.
- Lee, J.T.E., Dutta, N., Zhang, L., Tsui, T.T.H., Lim, S., Tio, Z.K., Lim, E.Y., Sun, J., Zhang, J., Wang, C.-H., Ok, Y.S., Ahiring, B.K., Tong, Y.W., 2022. Bioaugmentation of Methanosarcina thermophila grown on biochar particles during semi-continuous thermophilic food waste anaerobic digestion under two different bioaugmentation regimes. *Bioresour. Technol.* 360, 127590 <https://doi.org/10.1016/j.biortech.2022.127590>.
- Li, Wang, C., Xu, X., Sun, Y., Xing, T., 2022. Bioaugmentation with a propionate-degrading methanogenic culture to improve methane production from chicken manure. *Bioresour. Technol.* 346, 126607. [10.1016/j.biortech.2021.126607](https://doi.org/10.1016/j.biortech.2021.126607).
- Li, L., He, Q., Ma, Y., Wang, X., Peng, X., 2015a. Dynamics of microbial community in a mesophilic anaerobic digester treating food waste: relationship between community structure and process stability. *Bioresour. Technol.* 189, 113–120. <https://doi.org/10.1016/j.biortech.2015.04.015>.
- Li, Z.-Y., Inoue, D., Ike, M., 2023. Mitigating ammonia-inhibition in anaerobic digestion by bioaugmentation: a review. *J. Water Process Eng.* 52, 103506 <https://doi.org/10.1016/j.jwpe.2023.103506>.
- Li, Q., Qiao, W., Wang, X., Takayanagi, K., Shofie, M., Li, Y.-Y., 2015b. Kinetic characterization of thermophilic and mesophilic anaerobic digestion for coffee grounds and waste activated sludge. *Waste Manag.* 36, 77–85. <https://doi.org/10.1016/j.wasman.2014.11.016>.
- Li, Y., Zhang, Y., Sun, Y., Wu, S., Kong, X., Yuan, Z., Dong, R., 2017. The performance efficiency of bioaugmentation to prevent anaerobic digestion failure from ammonia and propionate inhibition. *Bioresour. Technol.* 231, 94–100. <https://doi.org/10.1016/j.biortech.2017.01.068>.
- Linsong, H., Lianhua, L., Ying, L., Changrui, W., Yongming, S., 2022. Bioaugmentation with methanogenic culture to improve methane production from chicken manure in batch anaerobic digestion. *Chemosphere* 303, 135127. <https://doi.org/10.1016/j.chemosphere.2022.135127>.
- Liu, C., Huang, H., Duan, X., Chen, Y., 2021. Integrated metagenomic and metaproteomic analyses unravel ammonia toxicity to active methanogens and syntrophs, enzyme synthesis, and key enzymes in anaerobic digestion. *Environ. Sci. Technol.* 55, 14817–14827. <https://doi.org/10.1021/acs.est.1c00797>.
- Mao, C., Feng, Y., Wang, X., Ren, G., 2015. Review on research achievements of biogas from anaerobic digestion. *Renew. Sustain. Energy Rev.* 45, 540–555. <https://doi.org/10.1016/j.rser.2015.02.032>.
- Möller, K., Müller, T., 2012. Effects of anaerobic digestion on digestate nutrient availability and crop growth: a review: digestate nutrient availability. *Eng. Life Sci.* 12, 242–257. <https://doi.org/10.1002/elsc.201100085>.
- Tian, H., Fotidis, I.A., Mancini, E., Angelidaki, I., 2017. Different cultivation methods to acclimatise ammonia-tolerant methanogenic consortia. *Bioresour. Technol.* 232, 1–9. <https://doi.org/10.1016/j.biortech.2017.02.034>.
- Tian, H., Fotidis, I.A., Mancini, E., Treu, L., Mahdy, A., Ballesteros, M., González-Fernández, C., Angelidaki, I., 2018. Acclimation to extremely high ammonia levels in continuous biometathation process and the associated microbial community dynamics. *Bioresour. Technol.* 247, 616–623. <https://doi.org/10.1016/j.biortech.2017.09.148>.
- Venkiteshwaran, K., Milferstedt, K., Hamelin, J., Zitomer, D.H., 2016. Anaerobic digester bioaugmentation influences quasi steady state performance and microbial community. *Water Res.* 104, 128–136. <https://doi.org/10.1016/j.watres.2016.08.012>.
- Wang, H., Fotidis, I.A., Angelidaki, I., 2015. Ammonia effect on hydrogenotrophic methanogens and syntrophic acetate-oxidizing bacteria. *FEMS Microbiol. Ecol.* 91, fiv130. [10.1093/femsec/fiv130](https://doi.org/10.1093/femsec/fiv130).
- Wang, H.-Z., Lv, X.-M., Yi, Y., Zheng, D., Gou, M., Nie, Y., Hu, B., Nobu, M.K., Narihiro, T., Tang, Y.-Q., 2019. Using DNA-based stable isotope probing to reveal novel propionate- and acetate-oxidizing bacteria in propionate-fed mesophilic anaerobic chemostats. *Sci. Rep.* 9, 17396. <https://doi.org/10.1038/s41598-019-53849-0>.
- Wang, S., Wang, Z., Usman, M., Zheng, Z., Zhao, X., Meng, X., Hu, K., Shen, X., Wang, X., Cai, Y., 2023. Two microbial consortia obtained through purposive acclimatization as biological additives to relieve ammonia inhibition in anaerobic digestion. *Water Res.* 230, 119583 <https://doi.org/10.1016/j.watres.2023.119583>.

- Wood, J.M., 2015. Bacterial responses to osmotic challenges. *J. Gen. Physiol.* 145, 381–388. <https://doi.org/10.1085/jgp.201411296>.
- Woraruthai, T., Supawatkorn, C., Uthapaisanwong, P., Kusunmano, K., Wongsurawat, T., Jenjaroenpun, P., Chaiyen, P., Wongnate, T., 2024. Isolation and characterization of *Enterococcus faecalis* isolate VT-H1: a highly efficient hydrogen-producing bacterium from palm oil mill effluent (POME). *Int. J. Hydrog. Energy* 49, 295–309. <https://doi.org/10.1016/j.ijhydene.2023.08.017>.
- Yan, M., Fotidis, I.A., Tian, H., Khoshnevisan, B., Treu, L., Tsapekos, P., Angelidaki, I., 2019. Acclimatization contributes to stable anaerobic digestion of organic fraction of municipal solid waste under extreme ammonia levels: focusing on microbial community dynamics. *Bioresour. Technol.* 286, 121376 <https://doi.org/10.1016/j.biortech.2019.121376>.
- Yang, Z., Guo, R., Xu, X., Wang, L., Dai, M., 2016. Enhanced methane production via repeated batch bioaugmentation pattern of enriched microbial consortia. *Bioresour. Technol.* 216, 471–477. <https://doi.org/10.1016/j.biortech.2016.05.062>.
- Zhang, H., Yuan, W., Dong, Q., Wu, D., Yang, P., Peng, Y., Li, L., Peng, X., 2022. Integrated multi-omics analyses reveal the key microbial phylotypes affecting anaerobic digestion performance under ammonia stress. *Water Res.* 213, 118152 <https://doi.org/10.1016/j.watres.2022.118152>.
- Zhang, L., Zhu, K., Li, A., 2016. Differentiated effects of osmoprotectants on anaerobic syntrophic microbial populations at saline conditions and its engineering aspects. *Chem. Eng. J.* 288, 116–125. <https://doi.org/10.1016/j.cej.2015.11.100>.
- Zhao, W., Chen, Z., Xia, D., Lv, Q., Li, S., 2023. Biogas production characteristics of lignite and related metabolic functions with indigenous microbes from different coal seams. *Fuel* 349, 128598. <https://doi.org/10.1016/j.fuel.2023.128598>.
- Ziganshina, E.E., Ziganshin, A.M., 2022. Anaerobic digestion of chicken manure in the presence of magnetite, granular activated carbon, and biochar: operation of anaerobic reactors and microbial community structure. *Microorganisms* 10, 1422. <https://doi.org/10.3390/microorganisms10071422>.